

SUPPLEMENTARY MATERIAL

Self-heating of biochar during postproduction storage by O₂ chemisorption at low temperatures

Aekjuthon Phounglamcheik^{1,2,*}, Nils Jonhson¹, Norbert Kenzle³, Christoph Strasser³, and Kentaro Umeki^{1,*}

¹Division of Energy Science, Luleå University of Technology, 971 87 Luleå, Sweden

²Material Science and Environmental Engineering, Tampere University, 33720 Tampere, Finland

³BEST - Bioenergy and Sustainable Technologies GmbH, Inffeldgasse 21b, 8010, Graz, Austria

S1. Detail of kinetic parameters measurement and calculation

Figure S1 depicts an example of mass loss curves obtained from TGA for the determination of kinetic parameters. The example shows three repetitions measured at isothermal temperatures of 50, 150, and 300 °C.

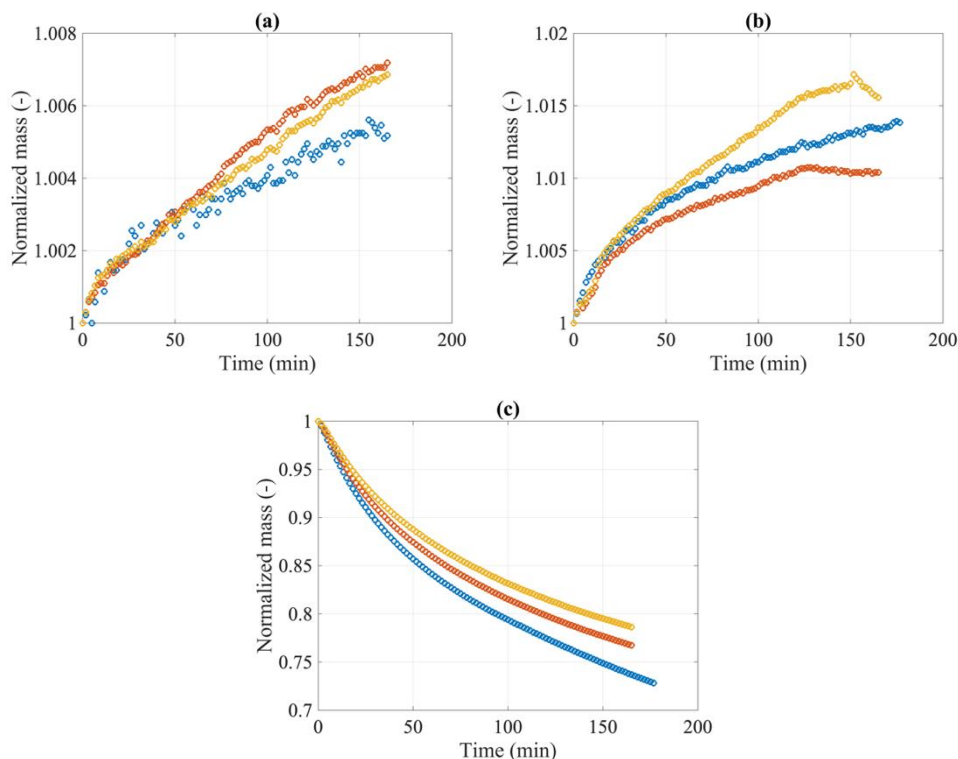


Figure S1. TG curves a) 50 °C and 20% O₂ b) 150 °C and 10% O₂ c) 300 °C and 5% O₂.

Figure S2 depicts the fitting of reaction rates for Reaction 1 and Reaction 2. The figure shows a reasonable fit by applying a first-order reaction equation.

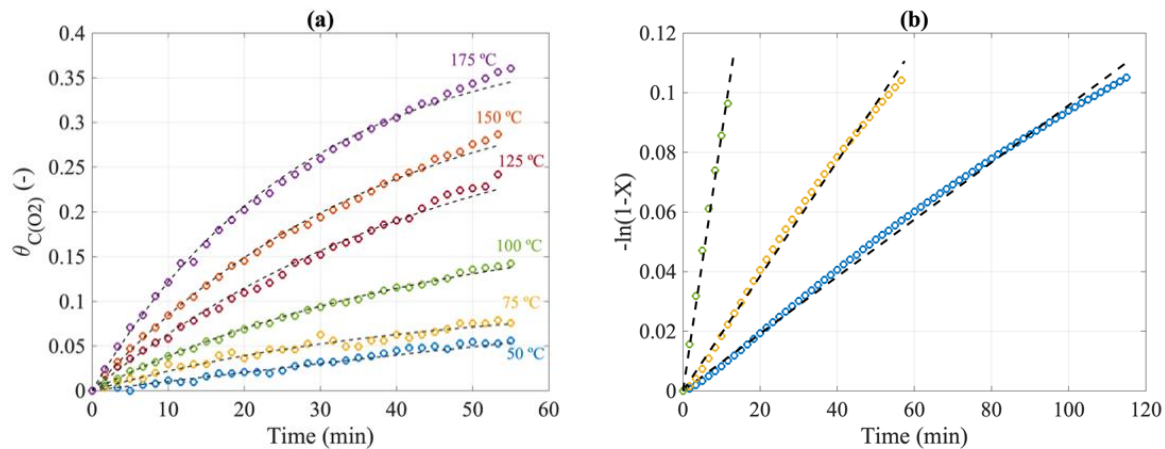


Figure S2. Fitting of Reaction 1 (a) and 2 (b). (Symbol: experiment, line: model)

The fitted rate constants are summarized in Table S1.

Table S1. Fitted rate constants.

| Temperature (°C) | k_{If} (1/s/bar) | | |
|---------------------|-----------------------|------------------------|-----------------------|
| | 5% O ₂ | 10% O ₂ | 20% O ₂ |
| 50 | 4.37x10 ⁻⁴ | 2.40x10 ⁻⁴ | 1.82x10 ⁻⁴ |
| 75 | 7.48x10 ⁻⁴ | 4.04 x10 ⁻⁴ | 1.76x10 ⁻⁴ |
| 100 | 1.52x10 ⁻³ | 6.24x10 ⁻⁴ | 4.09x10 ⁻⁴ |
| 125 | 2.20x10 ⁻³ | 1.35x10 ⁻³ | 5.21x10 ⁻⁴ |
| 150 | 2.86x10 ⁻³ | 1.79x10 ⁻³ | 6.93x10 ⁻⁴ |
| 175 | 4.75x10 ⁻³ | 2.07x10 ⁻³ | 1.51x10 ⁻³ |
| Temperature (°C) | k_{Ib} (1/s) | | |
| | 5% O ₂ | 10% O ₂ | 20% O ₂ |
| 50 | 2.44x10 ⁻⁵ | 3.46x10 ⁻⁵ | 4.07x10 ⁻⁵ |
| 75 | 5.63x10 ⁻⁶ | 2.41x10 ⁻⁶ | 4.16x10 ⁻⁵ |
| 100 | 2.30x10 ⁻⁴ | 1.75x10 ⁻⁵ | 1.76x10 ⁻⁵ |
| 125 | 2.65x10 ⁻⁴ | 2.56x10 ⁻⁴ | 4.89x10 ⁻⁴ |
| 150 | 3.36x10 ⁻⁴ | 3.57x10 ⁻⁴ | 9.25x10 ⁻⁴ |
| 175 | 3.38x10 ⁻⁴ | 4.92x10 ⁻⁴ | 5.24x10 ⁻⁴ |
| Temperature (°C) | k_2 (1/s) | | |
| | 5% O ₂ | 10% O ₂ | 20% O ₂ |
| 250 | 1.15x10 ⁻⁵ | 1.99x10 ⁻⁵ | 2.21x10 ⁻⁵ |
| 275 | 3.82x10 ⁻⁵ | 4.29x10 ⁻⁵ | 4.85x10 ⁻⁵ |
| 300 | 1.04x10 ⁻⁴ | 1.09x10 ⁻⁴ | 1.19x10 ⁻⁴ |

Kinetic parameters were optimized by using the following equation

$$\text{objective function} = \sum_{j=1}^{N_{exp}} \frac{\sum_{i=1}^{N_{data}} \frac{k_{exp} - k_{model}}{k_{exp}}}{N_{data}}, \quad (\text{S1})$$

where, N_{data} is the number of experimental data. This step was done using MATLAB's built-in function called fminsearch. Figure S3 shows reaction rates as a function of temperature between experimental data and the model.

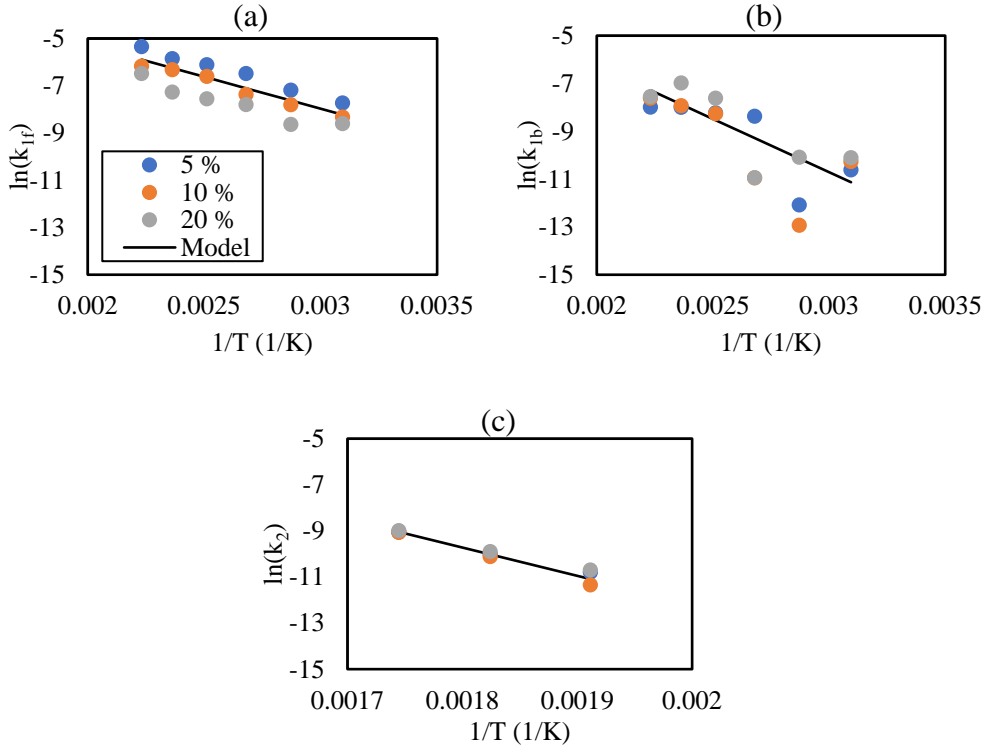


Figure S3. The Arrhenius plots for k_{if} (a), k_{ib} (b), and k_2 (c).

S2. Sensible heat and specific heat capacity

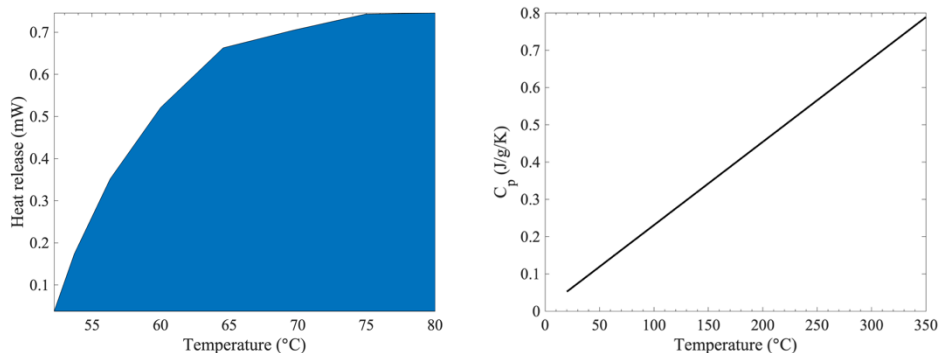


Figure S4. Sensible heat (a) and specific heat capacity (b) of biochar.

S3. Sub-models for physical properties implemented in the numerical model

Table S2. Values and correlations for physical properties

| Property | Correlation/value | Refs. |
|--|---|-------|
| Atmospheric pressure, Pa | $P_{atm} = 101325$ | - |
| Wind speed, m s ⁻¹ | $u_{wind} = 1$ | - |
| Bed pore diameter, mm | $d_{pore} = 10$ | - |
| Tortuosity of char bed, - | $\tau = 1/\sqrt{\varepsilon}$ | [1] |
| Permeability of char bed, - (Carman-Kozeney equation) | $\varphi = \frac{d_{pore}^2 \varepsilon^3}{180 \cdot (1 - \varepsilon^2)}$ | [2] |
| Reynolds number, - | $Re = \frac{2 \cdot u_{wind} \cdot bag\ width}{\mu_{air}}$ | - |
| Prandtl number, - | $Pr = \frac{\alpha_{air}}{D_{AB}}$ | - |
| Schmidt number, - | $Sc = \frac{\mu_{air}}{D_{AB}}$ | - |
| Nusselt number, - | $Nu = 0.332 \cdot \sqrt{Re} \cdot \sqrt[3]{Pr}$ | - |
| Sherwood number, - | $Sh = 0.332 \cdot \sqrt{Re} \cdot \sqrt[3]{Sc}$ | - |
| Effective diffusivity of gas mixture, m ² s ⁻¹ | $D_{mix} = (1 - x_A) \left(\sum \frac{x_i}{D_{Ai}} \right)$ | [3] |
| Specific heat capacity of gas | $\frac{C_{p,i}}{R} = a_1 T^{-2} + a_2 T^{-1} + a_3 + a_4 T + a_5 T^2 + a_6 T^3 + a_7 T^4$ | [4] |
| Dynamic viscosity of gases, kg m ⁻² s ⁻¹ | $\mu_{N2} = -0.0001T^2 + 0.4428T + 60.145 \times 10^{-7}$ $\mu_{CO2} = (0.3794T + 38.631) \times 10^{-7}$ $\mu_{O2} = (-8 \times 10^5)T^2 + 0.488T + 75.521 \times 10^{-7}$ | [5] |
| Thermal conductivity of gases, W m ⁻¹ K ⁻¹ | $\lambda_{CO2} = (0.0782T - 6.7926) \times 10^{-3}$ $\lambda_{N2} = (0.0532T + 11.861) \times 10^{-3}$ $\lambda_{O2} = (0.0605T + 9.7264) \times 10^{-3}$ | [5] |

S4. Evaluation of intraparticle effectiveness factor

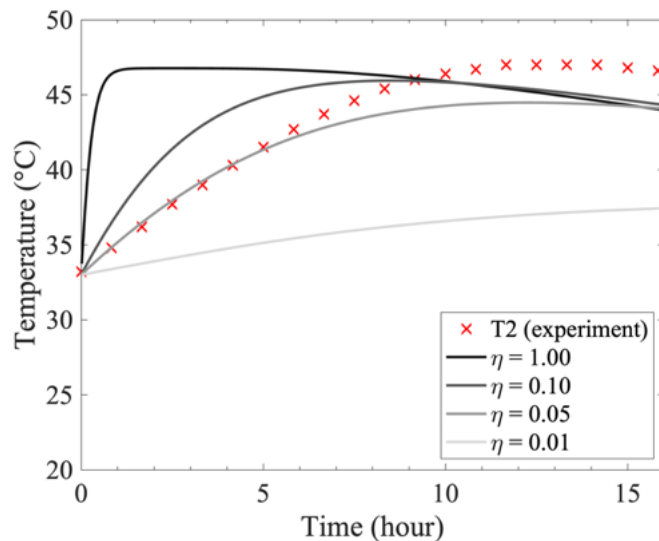


Figure S5. Effect of intraparticle effectiveness factor on time of self-heating.

References

- [1] Bruggeman DAG. Berechnung verschiedener physikalischer Konstanten von heterogenen Substanzen. I. Dielektrizitätskonstanten und Leitfähigkeiten der Mischkörper aus isotropen Substanzen. Annalen Der Physik 1935.
- [2] Kobe KA. Unit operations of chemical engineering (McCabe, W.L., and Smith, J.L.). Journal of Chemical Education 1957;34.
- [3] EUROKIN spreadsheet on requirements for measurement of intrinsic kinetics in the gas-solid fixed-bed reactor, 2012.
- [4] McBride BJ, Zehe MJ, Gordon S. NASA Glenn coefficients for calculating thermodynamic properties of individual species: National Aeronautics and Space Administration. John H Glenn Research Center at Lewis Field 2002.
- [5] Incopera FP, Dewitt DP, Bergman TL, Lavine AS. Fudamental Of Heat And Mass Transfer 6th Edition. vol. 53. 2013.